

61

# Exact hard-disk free volumes<sup>a)</sup>

William G. Hoover<sup>b)</sup>

*Department of Applied Science, University of California at Davis/Livermore and Lawrence Livermore Laboratory, Livermore, California 94550*

Nathan E. Hoover and Kenton Hanson<sup>c)</sup>

*University of California, Berkeley, California 94720*  
(Received 2 November 1978)

Properties of exact hard-disk free volumes are determined by a combination of analytical and numerical techniques. Both the high-density fluid phase and the lower-density fluid phase are treated. These one-particle free volumes are used to verify known thermodynamic information for hard disks and to calculate the shear modulus for the hard-disk solid phase. The free volumes are also compared to approximate free-volume estimates made from the known hard-disk entropy. The statistical distributions of free volume and free surface (perimeter of the free volume) are studied. The percolation transition, at which the free-volume changes from extensive to intensive, is found to occur at about one-third of the freezing density.

## I. INTRODUCTION

About 40 years ago, the concept of "free volume" was introduced into the statistical mechanics of liquids.<sup>1,2</sup> This free volume, the space available to a particle with its neighbors held fixed, was at first expected to play an important role in understanding fluid motion and structure. However, the semiquantitative theory of fluids which now exists<sup>3</sup> is not based on these simple ideas but rather on the perturbation description of fluids based upon the geometrical structure of the hard-sphere fluid. This structure has in turn been well characterized as a result of molecular dynamics and Monte Carlo computer experiments. Nevertheless, the expectation that a free-volume approach will ultimately prove successful is responsible for a continuing interest in free volumes. Recently, free-volume calculations using a relatively realistic soft potential have been carried out.<sup>4</sup>

The development of the Monte Carlo method led to the realization that, at least from a static, time-averaged viewpoint, a cell view of fluid structure is basically correct.<sup>5</sup> In the Monte Carlo simulations, it is usual, but not obligatory, to choose moving particles either sequentially or randomly. Another equally valid method is to move each particle several times before passing on to the next. In such a case, the Monte Carlo chain samples single-particle "cells," the localized regions in space to which dense-fluid particles are confined by their neighbors. The independence of the Monte Carlo pressure and energy averages to the sampling scheme guarantees that these cell-like pressure and energy averages are numerically identical (within the statistical fluctuations) to averages with the more conventional se-

quential or random choices for moving particles. A second way of viewing the cell-like sampling was discussed at length in Ref. 5: Let one of the particles in a classical many-body system have a much smaller mass than the rest. This light particle will then move much more rapidly than its more-massive neighbors, and will sweep out a localized free volume. This free volume will be, on the average, identical to that determined by cell-like Monte Carlo sampling. Thus, the pressure and energy can be determined exactly by appropriate averages of one-particle cell quantities. The relation of one-particle to many-particle theories of fluids was foreshadowed by exact relations discovered in the 1960's.<sup>6,7</sup> It was found that the exact many-body chemical potential could be determined from the small- $r$  limit of the pair distribution function.

In this paper, we set out to characterize the free volumes for hard disks (two-dimensional hard spheres) in a quantitative way. The two-dimensional problem can be analyzed more completely than the three-dimensional hard-sphere problem. In particular, the two-dimensional free volumes can be studied over the entire range of densities. Our three-dimensional hard sphere results are restricted, by geometrical complications, to fluid states at, or very near, the freezing density.<sup>8</sup>

The research discussed here has three goals:

- (1) Relating thermodynamic information to free volumes: Approximate cell theories suggest that free energy and entropy should give estimates of dense-fluid free volumes. We test such models for a case (hard disks) in which the underlying thermodynamic properties are well known.
- (2) Determining the hard-disk shear modulus: The one-particle cell picture can be used in either the solid or the fluid phase. The equivalence of cell-like sampling and the more conventional sequential or random methods allows us to calculate the hard-disk shear modulus by sampling one-particle cells in a system undergoing shear.
- (3) Understanding the transition of the free volume from a high-density intensive quantity to a low-density extensive quantity.

<sup>a)</sup>This work was performed under the auspices of the Department of Energy under contract No. W-74 05-ENG-48.  
<sup>b)</sup>Fulbright-Hayes Grantee, 1977-1978. A part of this work was carried out at the Australian National University. M. R. Osborne and R. O. W. Watts provided office space and computer time at the A.N.U. Computer Center.  
<sup>c)</sup>Materials and Molecular Research Division, Lawrence Berkeley Laboratory; supported by the Division of Materials Science, Office of Basic Energy Sciences, United States Department of Energy.

There is an interesting connection between this free-volume transition and the formation of critical-point clusters in a low-density gas.

The organization of the paper is as follows: In Sec. II, we define and measure the hard-disk free volume as a function of density. We then discuss simple intuitive models relating free volumes to thermodynamic quantities and compare the Monte Carlo results to the model predictions. In Sec. III, we consider the connection between the free volumes in a sheared system and the shear modulus for hard disks. The shear moduli are compared to simple cell-model predictions. In Sec. IV, we discuss the free-volume transition, from intensive to extensive, and compare the transition density found with related numerical work and with a simple intuitive model for critical clustering.

## II. FREE VOLUMES

Two different kinds of free volumes have been defined and used for hard particles. One of these is the space  $v_f^*$  available throughout the system for a new particle. At high density, this free volume is the union of many "holes" distributed throughout the system.  $v_f^*$  is extensive at any density and it has been shown to give a direct measure of the constant-volume chemical potential relative to an ideal gas<sup>6,7,9</sup>

$$\mu^e/kT = \ln(V/v_f^*). \quad (1)$$

Adams<sup>9</sup> has recently verified that this relation (1) provides a useful means of determining hard-sphere chemical potentials for densities up to half the close-packed density.

If we ask, alternatively, how much space is available to a particle already existing in the system, the answer  $v_f$  is extensive only at low density (when most free volumes span the entire volume available to the system). In the dense fluid, the free volume  $v_f$  is localized—it is a single hole—to a region in the immediate neighborhood of the particle considered. It is evident that, at some density (determined precisely in Sec. IV),  $v_f$  undergoes a transition, from intensive to extensive. At higher densities,  $v_f$  is the volume of the intuitive cell-theory free volume while  $v_f^*$ , a union of holes, remains extensive. (The difficulties involved in defining localized volumes for smooth potentials are discussed in Ref. 4.)

In Ref. 5, it is pointed out that the free volume for existing particles is simply related to the thermodynamic pressure

$$pV/NkT = 1 + (\sigma/2D)\langle s_f/v_f \rangle. \quad (2)$$

$p$ ,  $V$ ,  $N$ ,  $k$ , and  $T$  are, respectively, pressure, volume, number of particles, Boltzmann's constant, and the absolute temperature.  $\sigma$  is the particle diameter and  $D$  the number of dimensions (two for disks and three for spheres).  $v_f$  is the free volume available to a particle—the volume of the hole in which that particle is located.  $s_f$  is the surface area of that free volume ( $s_f$  is the perimeter in the two-dimensional hard-disk case). The relation (2) is derived by calculating the collision rate for a light particle confined to  $v_f$  and the contribution of such a particle to the momentum flux. Because classi-

cal particles make contributions to pressure and energy which are independent of mass, the light-particle contribution can alternatively be calculated by working out an average, indicated by brackets  $\langle \rangle$ , over all particles in an ordinary system with identical particles. The pressure is related to free-volume properties by Eq. (2). It can also be measured (via computer experiments) from the collision rate or by application of the virial theorem. Such direct estimates agree well with theoretically based pressures from the known seven-term hard-disk virial series and with high-density extrapolations of that series.<sup>10-14</sup>

In addition to the exact relation (2) between  $\langle s_f/v_f \rangle$  and pressure, there are approximate models linking the two. In the cell model,<sup>15</sup> the many-particle partition function is approximated by the  $N$ th power of a one-particle partition function. The configurational part of that one-particle partition function is then calculated (in what is called the "unsmoothed" cell model) by working out  $v_f$  for a lattice of perfectly ordered solid-phase particles. For disks, this lattice-based free volume shows a transition from intensive to extensive at one fourth the close-packed density. At that density, a disk can escape from its localized cell by squeezing between two of its confining neighbors. Differentiation of the cell-model free volume leads to an equation of state resembling Eq. (2) above, but with  $2D$  replaced by  $D$ . The fact that cell models do provide rough estimates of the pressure then suggests that the true  $\langle s_f/v_f \rangle$ , worked out for fluid-phase configurations rather than for the ordered-lattice configuration, will be roughly twice the size of  $s_f/v_f$  predicted by the cell model. Thus, we expect that the true free volumes are not only less regular than those of the ordered-lattice cell model, but also smaller in size. Cell model predictions of free energy<sup>16</sup> and the melting transition<sup>17</sup> have both proved to be surprisingly good.

Salsburg and his co-workers made a serious effort to improve upon the simple ordered-lattice cell model by introducing a systematic series of corrections. These correction terms correspond to allowing the simultaneous motion of two, three, four, etc. particles in a lattice of otherwise perfectly ordered neighbors. These attempts to improve the simple cell picture<sup>18,19</sup> appear to converge very slowly, particularly in two dimensions. More nearly accurate results, based on a self-consistent distribution of particles in ordered cells, have provided excellent free energy estimates—in the solid phase—for both disks and spheres.<sup>20</sup>

By following the geometric scheme outlined in Appendix, we have computed exact perimeters and free volumes for a series of hard-disk systems. Computer time limited the results to relatively small systems of 48 and 192 hard disks. Low-density comparisons of these small-system results with the exact Eq. (1) and the high-density comparison of 48-disk and 192-disk data at the same density suggest that the number dependence of  $s_f$  and  $v_f$  is small. As indicated in Appendix A, the free volumes for all  $N$  particles were analyzed after every  $10N$  accepted Monte Carlo moves. Typically, 50 different configurations were analyzed. Three

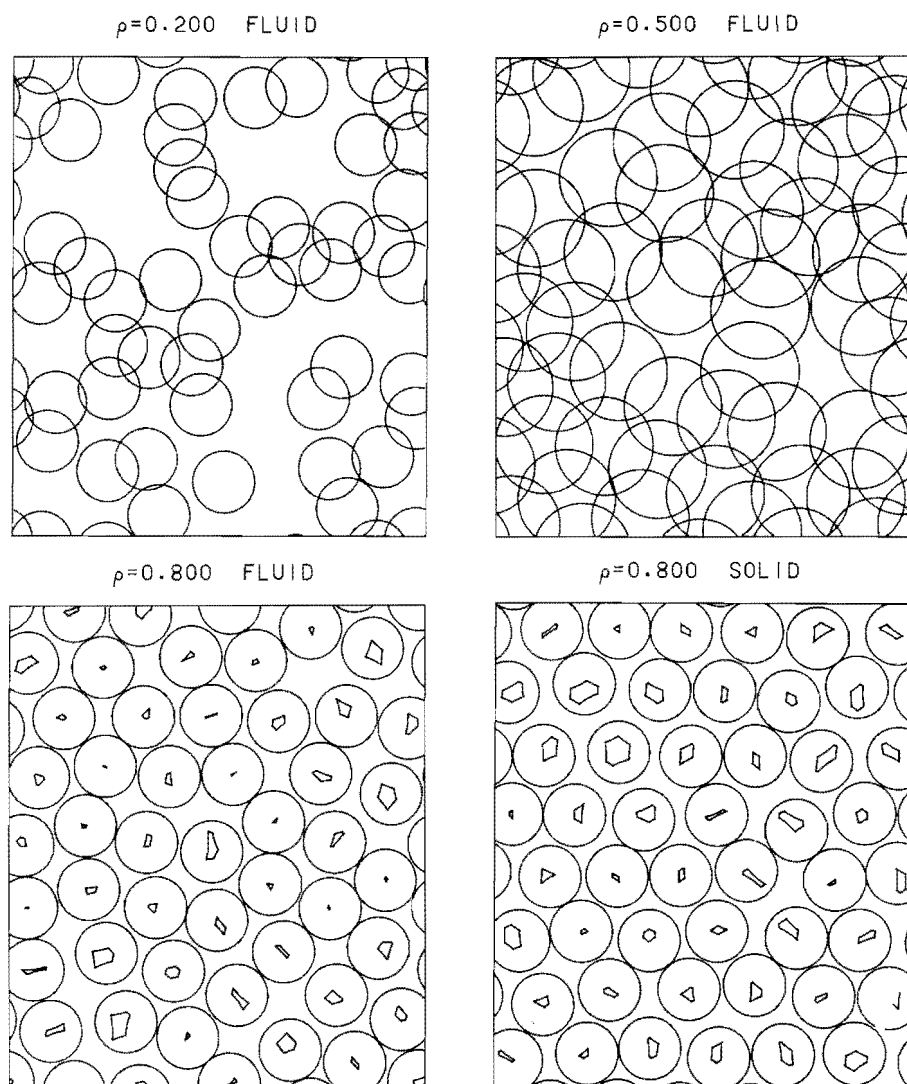


FIG. 1. Configurations of hard disks of diameter  $\sigma$  at densities of 0.2, 0.5, and 0.8 relative to close packing. At the two lower densities, "exclusion disks" of radius  $\sigma$  are drawn around each disk. These indicate the areas from which neighboring disks are excluded. At density 0.2, the disks form seven clusters and all 48 free volumes are extensive. At density 0.8, in both the fluid and the solid configurations, the free volumes have been drawn for each particle. These free volumes are small and intensive.

different regimes were encountered in the calculations:

- (1) extensive  $v_f$  and  $s_f$ —the low-density fluid;
- (2) dense fluid with intensive  $v_f$  and  $s_f$ ;
- (3) solid with intensive  $v_f$  and  $s_f$ .

Typical configurations illustrating the three regimes appear in Fig. 1. Numerical results, for a wide range of densities, are given in Table I. These results show that (as we had anticipated<sup>5</sup>) the fluid free volumes are smaller than the solid free volumes at the same density. This difference is caused by the relative packing inefficiency of the disordered and irregular fluid structure. Near the freezing density, there is an increase of about 20% in  $\langle v_f \rangle$  on going from the fluid to the solid phase.

The table contains two estimates for  $(Z-1)4/\sigma$ , where  $Z$  is the compressibility factor  $pV/NkT$  and  $\sigma$  is the hard-disk diameter. The first of these is  $\langle s_f/v_f \rangle$ , determined from the Monte Carlo data. The adjacent column is based on known large-system compressibilities for disks. The excellent agreement shows that the 48-disk system is sufficiently close to the thermodynamic limit for an accurate determination of the equation of state through Eq. (2) of the text.

The table also contains a check of the exact relation between the excess chemical potential and  $\ln \langle v_f' \rangle$  [Eq. (1)]. So long as  $v_f$  is in the low-density extensive regime, the 48-disk results should be described by the relation

$$\mu^e/kT = \ln V - \ln \langle v_f \rangle. \quad (3)$$

In the units of Table I, the volume per particle is  $(0.75)^{1/2}$  so that  $\ln(V)$  is 3.73. Table I confirms Eq. (3) for densities up to one fourth the close-packed density. Data for densities of 0.20, 0.25, and 0.30 (all relative to close packing) are somewhat unreliable. This is because the region associated with the intensive-extensive transition, discussed in Sec. IV, involves treating free volumes which, due to the periodic boundaries, span the system horizontally, vertically, or diagonally. The many special cases which arise in this intermediate region cannot all be handled by the methods described in Appendix. Accordingly, our numerical data are based on only those few configurations generated before such an exceptional case arose.

The table also makes it possible to check the ordered-lattice cell-model idea that the  $N$ th root of the configurational partition function corresponds to a single-particle

TABLE I. Comparison of Monte Carlo free-volume data with hard-disk thermodynamic quantities. These data (except as indicated) are for 50 48-disk or 25 192-disk configurations. The volume per particle is  $(0.75)^{1/2}$  so that  $\rho^{1/2}$  is the hard-disk diameter  $\sigma$ .  $Z$  is the compressibility factor  $pV/NkT$  and  $(Z-1)4/\sigma$  is the estimated value of  $\langle s_f/v_f \rangle$  for an infinite system. Our results are a few percent lower, primarily due to finite-system center-of-mass motion.<sup>13</sup> The low-density limiting value of  $\mu^e/kT + \ln\langle v_f \rangle$  approaches  $\ln(V)$ , i. e., 3.73 for 48 hard disks. For the solid infinite-system thermodynamic estimates, we used  $(S - S_{\text{cell}})/Nk = 0.05$  in the high-density limit.<sup>11,12</sup> The close-packed volume per disk is  $(0.75)^{1/2}\sigma^2$ . The triangular-lattice interparticle spacing  $d$  is the unit of length. The Monte Carlo jump length is  $\sigma[(V/V_0)^{1/2} - 1]$ .

$N$	$V_0/V$	$\langle s_f \rangle$	$\langle v_f \rangle$	$\langle s_f/v_f \rangle$	$(Z-1)4/\sigma$	$\ln\langle v_f \rangle$	$\mu^e/kT$	$\langle \ln v_f \rangle$	$S^e/Nk$
48	0.050	58.88	34.47	1.71	1.74	3.54	0.19	3.54	-0.09
48	0.100	73.29	27.91	2.63	2.67	3.33	0.41	3.33	-0.20
48	0.150	76.96	21.93	3.52	3.54	3.09	0.65	3.09	-0.31
48(12) <sup>a</sup>	0.200	71	16.7	4.41	4.46	2.81	0.92	2.79	-0.42
48(1) <sup>a</sup>	0.250	64	11	6	5.47	2.4	1.24	2.3	-0.56
48(4) <sup>a</sup>	0.300	18	3.7	6.5	6.61	1.22	1.60	0.88	-0.70
48	0.350	11.90	1.92	7.65	7.93	0.65	2.03	0.28	-0.86
48	0.400	6.97	1.00	9.25	9.49	-0.00	2.54	-0.38	-1.03
48	0.450	4.56	0.59	11.00	11.38	-0.53	3.14	-0.91	-1.23
48	0.500	3.31	0.37	13.26	13.71	-1.00	3.88	-1.38	-1.46
48	0.550	2.46	0.24	16.19	16.63	-1.43	4.80	-1.85	-1.72
48	0.600	1.858	0.155	19.64	20.38	-1.86	5.97	-2.30	-2.02
48	0.625	1.650	0.126	22.2	22.68	-2.07	6.68	-2.54	-2.20
48	0.650	1.417	0.0979	25.3	25.34	-2.32	7.49	-2.82	-2.38
48	0.675	1.249	0.0776	27.4	28.43	-2.56	8.43	-3.02	-2.59
48	0.700	1.067	0.0579	32.5	32.07	-2.85	9.53	-3.33	-2.82
48	0.725	0.943	0.0476	35.3	36.39	-3.05	10.82	-3.53	-3.07
48	0.750	0.849	0.0389	35.8	41.56	-3.25	12.35	-3.65	-3.35
48	0.775	0.727	0.0291	43.6	47.84	-3.54	14.20	-4.00	-3.67
48	0.800	0.624	0.0218	48.9	55.57	-3.83	16.46	-4.27	-4.04
48 <sup>b</sup>	0.800	0.680	0.0261	39.4	40.77	-3.64	13.06	-3.96	-3.95
48 <sup>b</sup>	0.850	0.498	0.0144	52.1	53.69	-4.24	16.96	-4.53	-4.59
48 <sup>b</sup>	0.900	0.321	0.0061	76.7	80.04	-5.10	24.44	-5.38	-5.46
48 <sup>b</sup>	0.950	0.158	0.0015	154.9	159.80	-6.50	45.83	-6.79	-6.89
192 <sup>b</sup>	0.900	0.319	0.0061	79.4	80.04	-5.11	24.44	-5.42	-5.46

<sup>a</sup>The uncertainty in  $v_f$  is typically 1%–2%. These entries are based on fewer configurations and are less accurate.

<sup>b</sup>These are single-occupancy solid-phase runs.

free volume. If this were so, then the logarithm of the free volume, in the units of Table I, should correspond to the excess entropy. The ordered-lattice cell model does not distinguish  $\langle \ln v_f \rangle$  from  $\ln\langle v_f \rangle$  because that model contains no cell-size fluctuations. In the table, we include both averages of the Monte Carlo data. Of the two,  $\ln\langle v_f \rangle$  is somewhat closer to the known entropy values than is  $\langle \ln v_f \rangle$  in the dense-fluid case.

In Fig. 2, the free-volume data are plotted as functions of density. We have also included the estimates of the configurational partition functions  $N$ th roots from the excess entropy and from the unsmoothed cell model. The figure illustrates a remarkably simple dependence of the dense-fluid free volumes on density. Both  $\ln\langle v_f \rangle$  and  $\langle \ln v_f \rangle$  vary almost linearly with density. Ichimura, Ogita, and Ueda found similar results for soft-core dense-fluid configurations in three dimensions (4). The approximate cell model, on the other hand, predicts a more complicated density dependence.

At each density, the fluctuations in free volume and perimeter can be used to identify exponents in the probability densities

$$P(x) \propto x^\alpha \exp(-\beta x^\gamma). \quad (4)$$

Meijering's work on the distribution of Voronoi–Polyhedra volumes and surfaces<sup>21</sup> suggested that the expo-

nent  $\gamma$  in Eq. (4) be chosen as 1 when  $x$  represents  $v_f$ , and 2 when  $x$  represents  $s_f$  in the probability density (4). Kiang<sup>22</sup> was able to verify such relations numerically, in both two and three dimensions, for random distributions of points.

The data gathered in the Monte Carlo runs suggest that the exponent  $\alpha$  in Eq. (4) is about 0.1 for  $v_f$  and about 0.6 for  $s_f$  in the dense fluid. We have not tabulated fluctuations in  $v_f$  and  $s_f$  as functions of density because the precision of the data does not warrant. The data suggest that  $\alpha$  increases slightly with density but more extensive calculations on larger systems would be required to establish this. If the free volume distribution at fixed density were an exponential one (with  $\alpha=0$ ), then the difference between  $\ln\langle v_f \rangle$  and  $\langle \ln v_f \rangle$  would be Euler's constant (0.577). The slightly smaller difference between the two Monte Carlo averages, 0.4 or so, corresponds to the small nonzero value of  $\alpha$ .

### III. ELASTIC CONSTANTS

The isothermal and adiabatic elastic constants can be derived from the partition function by differentiating twice with respect to the macroscopic thermodynamic strains.<sup>23</sup> The resulting ensemble averages involve the second derivative of the interparticle pair potential and the square of the first derivative. Because, for hard

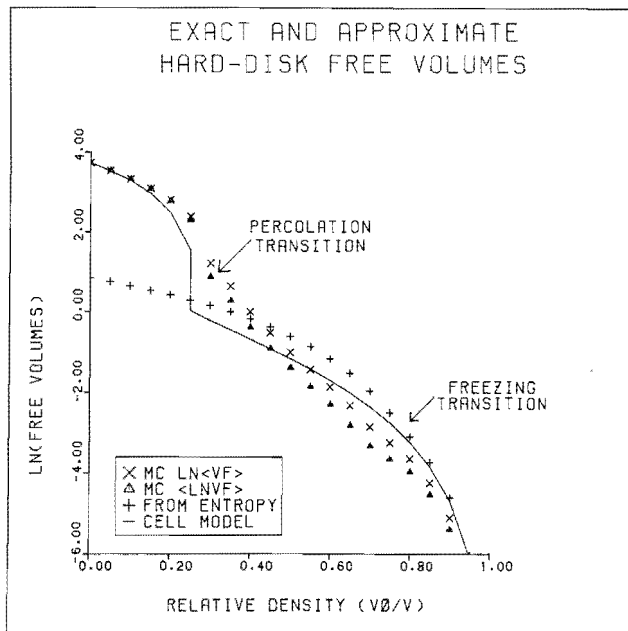


FIG. 2. Variation of the free volume  $v_f$  and excess entropy  $S^e$  with density for 48 hard disks. The excess entropy is that relative to an ideal gas at the same density and temperature. Thus, the approximation that  $S^e/Nk = \ln(v_f N/Ve) = \ln(v_f/d^2) - 0.856$  can be tested by plotting  $S^e/Nk + 0.856$  for comparison with the measured free volumes. The data can be described within about 0.1 by the straight line relation  $\ln(v_f/d^2) = 3.9 - 9.6\rho$ , where  $\rho$  is the density relative to close packing. We also show the unsmoothed cell model approximation to  $\ln(v_f/d^2)$ . The cell model predicts a percolation transition density of one fourth the close packed density.

particles, both averages diverge, an alternative route to reach the elastic constants is desirable. Here we relate the hard-disk shear modulus to an averaged momentum transfer along the perimeter of the free volume.

Consider a crystal with an imposed macroscopic shear strain  $\epsilon_{xy}$ . If the particles in the crystal all interact with the same force law, then the contribution of every particle to the shear stress  $-p_{xy}$  is independent of that particle's mass. The virial theorem expression for the shear stress

$$-p_{xy} = \frac{1}{V} \sum_{i < j} \phi'(r_{ij}) x_{ij} y_{ij} / r_{ij} \quad (5)$$

can be converted to an integral of  $\sin\theta \cos\theta$  around the free-volume perimeter

$$p_{xy} V/NkT = \frac{1}{2} \sigma^2 \left\langle \sum_h \int \sin\theta_h \cos\theta_h d\theta_h / v_f \right\rangle, \quad (6)$$

where  $\theta$  is measured counterclockwise relative to the  $x$  axis. The  $\theta$  integrations in Eq. (6) are carried out in a series of coordinate systems centered on the 3 to 6 disks which contribute to the free-volume boundary of the particle being considered.

For two-dimensional crystals with hexagonal symmetry, the linear shear modulus is independent of orientation. For large strains, this symmetry is lost. Direct evaluation of the shear modulus, using Eq. (6) for relatively small strains, gives the shear-modulus estimates listed in Table II. Although the strains actually used in the Monte Carlo work may exceed the elastic limits for an infinite hard-disk crystal, unsmoothed cell-model calculations suggest that these finite-strain results should lie within about a percent of the zero-strain limit in which the linear moduli are defined. At strains somewhat smaller than those appearing in Table II, the pressure fluctuations are so severe that even the sign of  $-p_{xy}$  is uncertain. Our results, even at the large strains given in Table II, have uncertainties of several percent due to the relatively large statistical fluctuations in the Monte Carlo calculations.

There are several ways to estimate the shear modulus theoretically. The unsmoothed cell-model approximation to the Helmholtz free energy can be used to derive an expression similar to Eq. (6). Just as in the hydrostatic case, the cell-model modulus is calculated by omitting the 2 appearing in the exact relation (6). We have evaluated the cell-model shear modulus numerically, by using the Monte Carlo program written for the hard-disk calculation, and making a shear-modulus calculation before the particles undergo Monte Carlo displacements. The cell-model shear modulus (see Table II) is much too large. In three dimensions, even larger disparities between the cell-model and exact thermal shear moduli have been found in calculations using the Lennard-Jones and exponential-six potentials.<sup>23</sup>

TABLE II. Shear modulus  $\eta$  for hard disks from free volumes. In these Monte Carlo calculations, each disk is confined to a circular cell of diameter  $d$ . The macroscopic shear strain  $\epsilon_{xy} = du_x/dy$  was imposed with periodic boundaries. The Monte Carlo data are uncertain within about 20%. Comparisons with three approximate theoretical shear-modulus estimates (see Sec. III) appear in the last four columns. The two "harmonic" columns list half the isothermal and isentropic bulk moduli, respectively.

$N$	$V_0/V$	$\epsilon_{xy}$	$p_{xy}V/NkT$	$\eta V/NkT$	Cell	Cell cluster	Harmonic
48	0.850	0.020	-0.77	38	71	35	44 or 133
192	0.850	0.020	-1.03	52	71	35	44 or 133
48	0.900	0.010	-1.22	122	174	86	100 or 299
192	0.900	0.010	-1.37	137	174	86	100 or 299
48	0.950	0.005	-2.98	596	752	371	400 or 1197
192	0.950	0.005	-2.07	413	752	371	400 or 1197

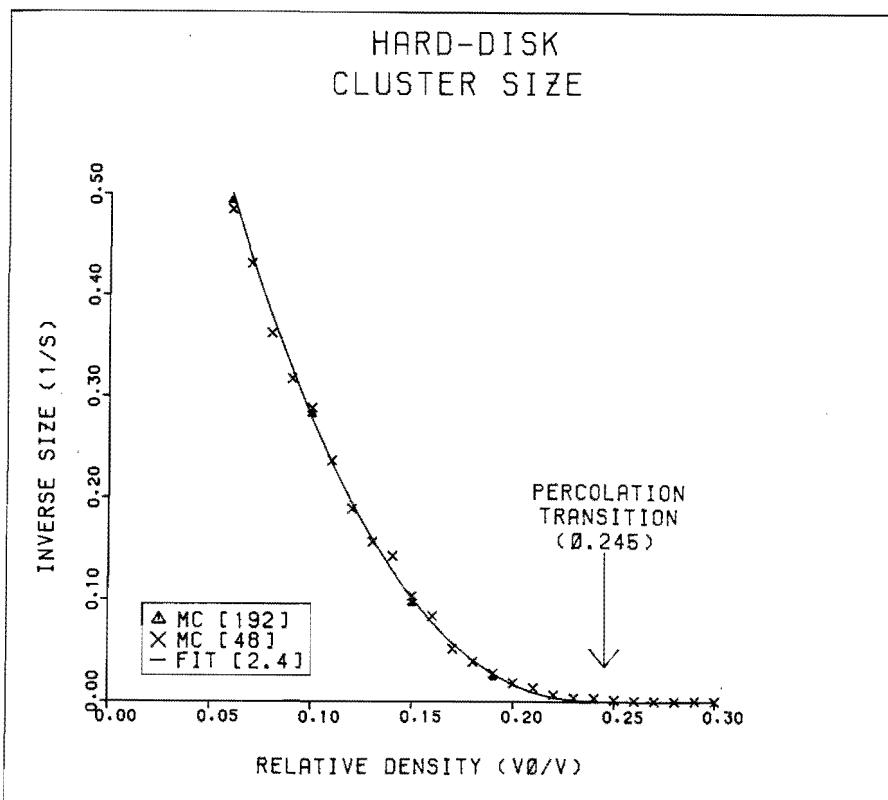


FIG. 3. Variation of average cluster size  $S$  with density. The low-density linear decrease is consistent with the partition functions calculated in Sec. IV. We show cluster-size data from Monte Carlo calculations (50 configurations at each density). The data have been adjusted by increasing the offset from the low-density limit  $[1 - (1/S)$  by  $N/(N-1)]$ . The fit to the data shown in the figure is  $1/S = 28.8 (\rho - 0.245)^{2.4}$ .

A second shear-modulus estimate can be based on the cell-cluster modification of the unsmoothed cell model. The cell-cluster theory computes formally exact corrections to the cell-model free energy. These corrections systematically account for particle correlations in clusters of two, three, etc. contiguous particles. Despite the fact that the three-particle cell-cluster correction is much larger than the already-large two-particle correction, the two corrections taken together produce a shear modulus in error by only 13%. This cell cluster theory prediction for the small-strain high-density shear modulus is equal to 0.494 times the unsmoothed-cell-model prediction. Because the theoretical finite-strain and finite-density corrections are unknown, we have used this same correction factor (0.494) to estimate "cell-cluster" shear moduli for Table II. A more reliable theoretical estimate could probably be obtained by extending Barker and Gladney's work<sup>20</sup> on the hard-disk pressure and free energy to the shear modulus.

A third shear-modulus estimate can be obtained by considering two-dimensional crystals in which the interactions are purely harmonic, and between nearest neighbors only. Then the shear modulus is equal to half the bulk modulus. Because the isothermal and isentropic bulk moduli for hard disks differ by about a factor of 3 (see Table II), this relation does not provide a precise estimate of the shear modulus. The Monte Carlo shear modulus lies closer to half the isothermal bulk modulus.

The Monte Carlo shear-modulus values make it possible to compute Poisson's ratio for hard disks, the ratio of transverse expansion to longitudinal compression

at constant pressure. In two dimensions, the maximum value of Poisson's ratio  $[(\lambda/(\lambda+2\eta))$  in terms of the Lamé constants] is unity, the value for an incompressible material; if the forces are harmonic, then this ratio is one third. For hard disks, the relatively great heating associated with isentropic compression gives a much larger Poisson's ratio than that found for isothermal compression.

#### IV. THE PHYSICAL-CLUSTER TRANSITION FOR HARD DISKS

In the low-density case, it is natural to consider the hard-disk system as being composed of clusters. A "cluster" of disks consists of  $j$  contiguous particles, each lying within a distance  $2\sigma$  (two hard-disk diameters) of at least one other disk in the cluster, and arranged in such a way that a continuous path can be traced between any pair of disks in the cluster, with no disk-to-disk gaps in the path larger than  $2\sigma$ .

At low enough density, it is possible to calculate the partition functions for clusters of 1, 2, 3, etc. disks, and, using the grand partition function, to calculate the number of such clusters as a function of density. Recent calculations for overlapping disks—disks which are allowed to interpenetrate freely—carry the partition-function calculations through terms of fourth order in the density.<sup>24</sup> For nonoverlapping disks, the calculation is more difficult, and we have not pursued it beyond the one- and two-disk terms given below in Eq. (7).

Following the partition-function notation introduced by Hill,<sup>25</sup> the configurational integrals for one- and two-disk clusters have the forms

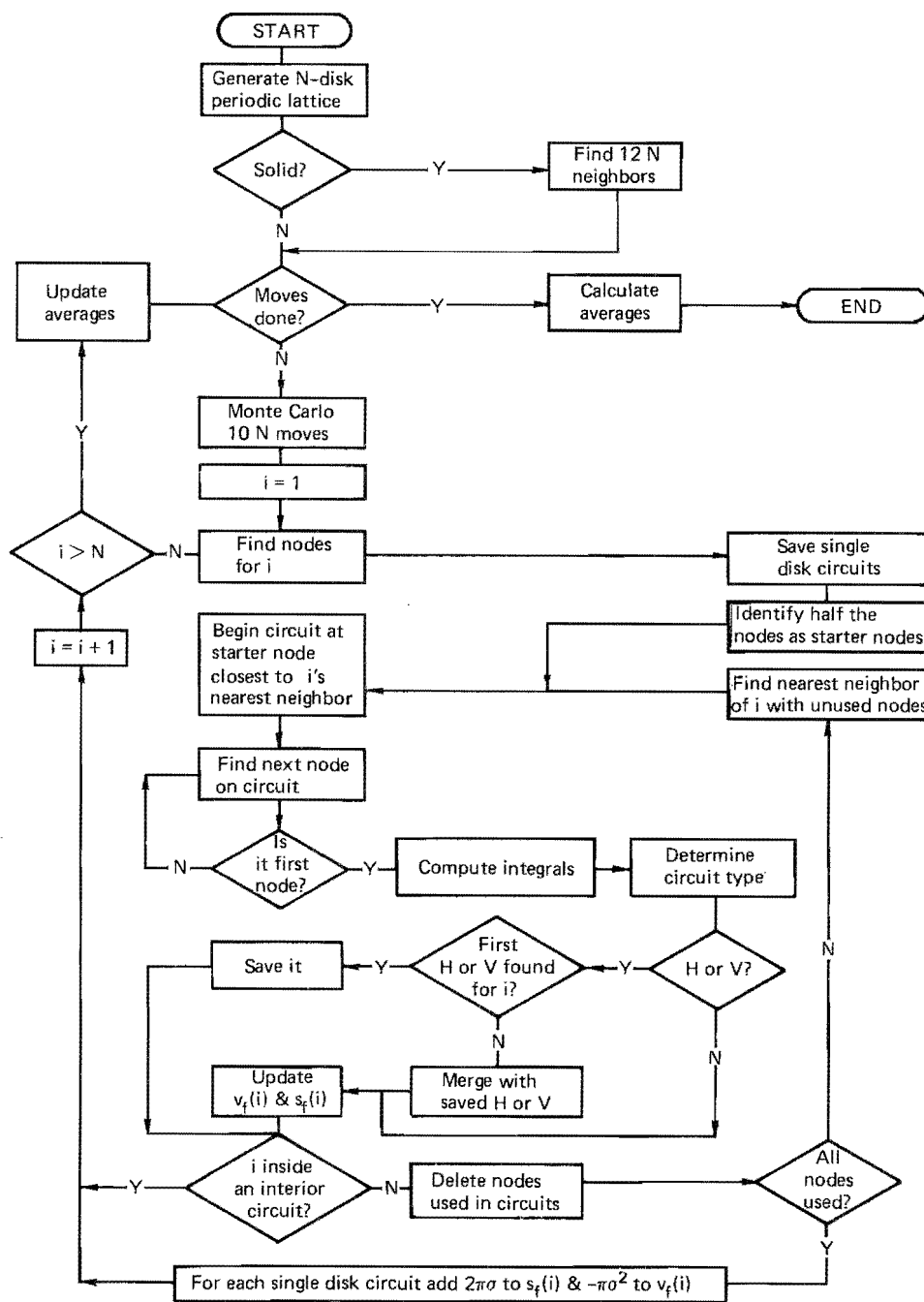


FIG. 4. Summary of the method used in our free-volume calculations.

$$\begin{aligned}
 Y_{10} &= V, \\
 Y_{20} &= V(V - 1.5B), \\
 Y_{01} &= V(1.5B).
 \end{aligned}
 \tag{7}$$

For ordinary hard disks, the second virial coefficient  $B$  is  $1.8138V_0$ . For the simpler model of overlapping disks,<sup>24</sup> the 1.5 in Eqs. (7) is replaced by 2. In either case, the cluster partition functions can be used<sup>24</sup> to predict the densities of one- and two-particle clusters. As density increases, the average cluster size grows. A transition—the “percolation” transition—is signaled by the divergence of the average cluster size.<sup>26–28</sup>

The average cluster size diverges, according to our Monte Carlo results, at a density of  $\rho_c = 0.245 \pm 0.02$ ,

relative to close packing. The estimate in Ref. 24, for disks which can interpenetrate, is as expected somewhat higher (0.32).

In the Monte Carlo calculations, we determined the average cluster size by finding  $j(i)$  for each particle in the system.  $j(i)$  is the number of particles making up the cluster in which particle  $i$  is found. The average of these  $j$ 's is the average cluster size  $S = \langle j \rangle$ . Figure 3 shows the variation of  $S$  with density. The data indicate a transition at a density of 0.245. At this density, the thermodynamic-limit probability for finding a particle in the largest cluster rises abruptly from zero.

At this density, a single macroscopic cluster spans the system and contains most of the particles. Thus,

$S$  is of order  $N$  rather than of order unity at, or above, the percolation-transition density. The percolation density found here agrees with a short extrapolation of the data of Pike and Seager.<sup>29</sup> Those authors used a method for generating configurations which is different from that used here for hard disks, but the difference is not an important one at the low densities they considered.

The increase of cluster size  $S$  with density is thought to vary as (about) the inverse 19/8 power of  $d\rho$ ,<sup>24,28,30</sup> where  $d\rho$  is the density difference relative to the percolation density. Our results are consistent with this exponent. A crude model predicting 20/8 can be constructed by considering the equilibrium between clusters of  $j$  and  $j+1$  particles at a density near the transition density. For dimensional reasons, we expect that the number of clusters of size  $j$  varies as  $N(\rho/\rho_c)^j$ .

Suppose also that the rates at which  $j$ -particle clusters grow (to  $j+1$ ) and at which  $(j+1)$ -particle clusters decay (to  $j$ ) are equal. This would be the expected consequence of detailed balance between these two cluster types. If the growth and decay terms are proportional to surface area, to  $j^{1/2}$  and to  $(j+1)^{1/2}$ , respectively, then a balance in rates suggests that the number of clusters varies as  $j^{-1/2}$  and  $(j+1)^{-1/2}$ . The estimate

$$N_j \approx N(\rho/\rho_c)^j / j^{1/2} \quad (8)$$

for  $N_j$ , then allows us to calculate the dependence of  $S$  on density by integrating  $j^2$  over the distribution (8). (Because each  $j$ -particle cluster contains  $j$  particles, such a cluster contributes  $j^2$  to  $S$ .)

The integration over  $j$  gives the result

$$S \equiv \langle j^2 \rangle \approx N(\rho_c/\delta\rho)^{5/2} \approx N/d\rho^{5/2}. \quad (9)$$

Fisher<sup>27</sup> outlines a slightly different approximate model which is closer to numerical estimates of the transition density dependence of  $S$  in three dimensions<sup>24</sup> but less close in two dimensions.

## V. REMARKS

The data given here characterize quantitatively the available one-particle states in a hard-disk system. The free-volume distribution at each density is approximately exponential, as is also the dependence of the average free volume on density. These two results should serve as useful guides in constructing and improving cell theories of the fluid state.<sup>31</sup> Neither of these simple relations has so far been predicted theoretically.

## APPENDIX

The free volumes are calculated by first locating, for each configuration to be analyzed, the "nodes" formed by the intersections of pairs of "exclusion disks" of radius  $\sigma$ . Ordered (by angle) pairs of these nodes are

then connected together to make "circuits" and the areas and perimeters of the circuits are expressed as polar-coordinate integrals. The periodic boundary conditions complicate the task but reduce the number dependence sufficiently to make their use essential. The flow chart is a summary of the method used in our free-volume calculations (Fig. 4).

- <sup>1</sup>H. Eyring and J. O. Hirschfelder, *J. Phys. Chem.* **41**, 249 (1937).
- <sup>2</sup>J. E. Lennard-Jones and A. F. Devonshire, *Proc. R. Soc. (London) Ser. A* **163**, 53 (1937); **165**, 1 (1938); **169**, 317 (1939); **170**, 464 (1939).
- <sup>3</sup>J. A. Barker and D. Henderson, *Rev. Mod. Phys.* **48**, 587 (1976).
- <sup>4</sup>T. Ichimura, N. Ogita, and A. Ueda, *J. Phys. Soc. Jpn.* **45**, 252 (1978).
- <sup>5</sup>W. G. Hoover, W. T. Ashurst, and R. Grover, *J. Chem. Phys.* **57**, 1259 (1972).
- <sup>6</sup>W. G. Hoover and J. C. Poirier, *J. Chem. Phys.* **37**, 1041 (1962).
- <sup>7</sup>B. Widom, *J. Chem. Phys.* **39**, 2808 (1963).
- <sup>8</sup>K. Hanson and W. G. Hoover (unpublished calculations).
- <sup>9</sup>D. J. Adams, *Mol. Phys.* **28**, 1241 (1974).
- <sup>10</sup>W. G. Hoover and B. J. Alder, *J. Chem. Phys.* **45**, 2361 (1966).
- <sup>11</sup>W. G. Hoover and F. H. Ree, *J. Chem. Phys.* **49**, 3609 (1968).
- <sup>12</sup>B. J. Alder, W. G. Hoover, and D. A. Young, *J. Chem. Phys.* **49**, 3688 (1968).
- <sup>13</sup>W. G. Hoover and B. J. Alder, *J. Chem. Phys.* **46**, 686 (1967).
- <sup>14</sup>K. W. Kratky, *Physica (Utrecht) A* **85**, 607 (1976).
- <sup>15</sup>R. J. Buehler, R. H. Wentorf, J. O. Hirschfelder, and C. F. Curtiss, *J. Chem. Phys.* **19**, 61 (1951).
- <sup>16</sup>L. V. Woodcock and K. Singer, *Trans. Faraday Soc.* **67**, 12 (1971).
- <sup>17</sup>B. J. Alder, W. G. Hoover, and T. E. Wainwright, *Phys. Rev. Lett.* **11**, 241 (1963).
- <sup>18</sup>F. H. Stillinger and Z. W. Salsburg, *J. Chem. Phys.* **46**, 3962 (1967).
- <sup>19</sup>F. H. Stillinger, Z. W. Salsburg, and R. L. Kornegay, *J. Chem. Phys.* **43**, 932 (1965).
- <sup>20</sup>J. A. Barker and H. M. Gladney, *J. Chem. Phys.* **63**, 3870 (1975).
- <sup>21</sup>J. L. Meijering, *Philips Res. Rep.* **8**, 270 (1953).
- <sup>22</sup>T. Kiang, *Z. Astrophys.* **64**, 433 (1966).
- <sup>23</sup>A. C. Holt, W. G. Hoover, S. G. Gray, and D. R. Shortle, *Physica (Utrecht)* **49**, 61 (1970).
- <sup>24</sup>S. W. Haan and R. Zwanzig, *J. Phys. A* **10**, 1547 (1977).
- <sup>25</sup>T. L. Hill, *J. Chem. Phys.* **23**, 617 (1955).
- <sup>26</sup>S. R. Broadbent and J. M. Hammersley, *Proc. Cambridge Philos. Soc.* **53**, 629, 642 (1957).
- <sup>27</sup>M. E. Fisher, *Rep. Prog. Phys.* **30**, 615 (1967).
- <sup>28</sup>J. W. Essam, *Phase Transitions and Critical Phenomena*, edited by C. Domb and M. S. Green (Academic, London, 1972), Vol. 2, Chap. 6.
- <sup>29</sup>G. E. Pike and C. H. Seager, *Phys. Rev. B* **10**, 1421, 1435 (1974).
- <sup>30</sup>I. Enting and W. T. Ashurst (stimulating conversations).
- <sup>31</sup>D. J. Adams and A. J. Matheson, *J. Chem. Soc. Faraday Trans. 2* **68**, 1536 (1972); and *Chem. Phys. Lett.* **22**, 484 (1973).